Polymer Bulletin (2020) 77:4417–4443
https://doi.org/10.1007/s00289-019-02971-0

ORIGINAL PAPER

Thermoresponsive cryogels of poly(2-hydroxyethyl methacrylate-*co*-*N*-isopropyl acrylamide) (P(HEMA-*co*-NIPAM)): fabrication, characterization and water sorption study

Anuja Jain[1] · Jaya Bajpai[1] · A. K. Bajpai[1] · Abhilasha Mishra[2]

Received: 3 July 2018 / Revised: 19 July 2019 / Accepted: 24 September 2019 /
Published online: 28 September 2019

Abstract

Cryogels of poly(2-hydroxyethyl methacrylate-co-*N*-isopropylacrylamide) (P(HEMA-*co*-NIPAM)) were prepared by cryogelation technique. Redox polymerization method was utilized to copolymerize monomers 2-hydroxyethyl methacrylate (HEMA) and *N*-isopropylacrylamide (NIPAM), using *N*, *N*′-methylene-bis-acrylamide (MBA) as cross-linker. Characterization of the as-prepared cryogels was done by Fourier-transform infrared spectroscopy, field emission scanning electron microscopy, differential scanning calorimetry, thermogravimetric analysis and X-ray diffraction techniques, respectively. During synthesis of cryogels, the concentrations of HEMA, NIPAM, MBA, redox initiator, and activator and the number of freezing–thawing cycles were varied to obtain different compositions of P(HEMA-*co*-NIPAM) cryogels. These cryogels were further evaluated for water sorption capacity through gravimetric method. The pH, temperature and nature of the swelling medium were also varied to observe their effects on water uptake capacity of the cryogels. The biocompatible nature of the materials was ascertained by blood hemolysis test. The prepared cryogels of P(HEMA-*co*-NIPAM) were found to be macroporous, have good water uptake potential, fair biocompatible, thermally stable nature, displayed temperature-sensitive water sorption behavior and thus showed potential to be utilized as scaffold in tissue engineering.

Keywords Copolymer · Cryogel · Characterization · Swelling · Blood compatibility

✉ A. K. Bajpai
akbmrl@yahoo.co.in

[1] Bose Memorial Research Laboratory, Department of Chemistry, Government Autonomous Science College, Jabalpur, MP 482001, India

[2] Department of Chemistry, Graphic Era University, Dehradun, Uttarakhand 248001, India

Introduction

Cryogels are macroporous hydrogels synthesized by the process of cryogelation [1]. This process involves the freezing (storing at sub-zero temperature) and thawing of monomer or polymeric material which lead to the formation of a gel which is often termed as 'cryogel' [2]. During the freezing process, the solvent changes into ice/solvent crystals, while the reactants are confined to an unfrozen or semi-frozen phases where they undergo polymerization and form a three-dimensional polymer network. On thawing the reaction mixture, the ice/solvent crystals melt thus forming interconnected macropores in the polymer network. Due to the presence of large interconnected pores, the cryogels can imbibe enormous quantity of water. They are soft, elastic and display characteristics similar to those of the living tissues [1]. They are biocompatible in nature and find applications in various fields such as enzyme immobilization [3, 4], chromatographic separation [5], tissue engineering [6], wound repair [7] and H_2 production [8]. Poly(2-hydroxyethyl methacrylate) (PHEMA) is a well-recognized biocompatible material [9] and has been vastly utilized for numerous applications such as wound dressing materials [10], contact lenses [11], drug delivery systems [12], and tissue engineering [13]. Cryogels based on HEMA have been largely synthesized and well characterized. Ingavle et al. [14] prepared poly(hydroxyethyl methacrylate) poly(HEMA) and poly(HEMA-*co*-ethyleneglycol diacrylate poly(HEMA-*co*-PEGDA) cryogels and judged their potential as matrices for removal of bio-toxins. Erzengin and coworkers [15] prepared Cu^{2+} appended sporopollenin particles and implanted them in P(HEMA) cryogels. The prepared cryogels were utilized for adsorption and purification of human serum albumin. In past few years, interests in smart hydrogels are on the steep rise. They are of stimuli-sensitive nature meaning that they exhibit large reversible changes in properties on being subjected to small alterations in their environment such as exposure to light, shift in temperature, variation in pH, biological factors or changes in magnetic/electrical fields [16]. The capability of hydrogels to exhibit changes in the properties in presence of the external stimuli makes them useful for biomedical applications. Smart polymers find applications in various fields such as tissue engineering, bio-sensing devices, and drug release systems. [16, 17].

Of late there has been a growing enthusiasm for smart materials which are thermoresponsive due to their huge potential in biomedical field. Thermo-sensitive hydrogels are responsive to alterations in temperature. They swell and deswell in aqueous solution below and above a definite temperature know as the lower critical solution temperature (LCST). One such thermo-sensitive polymer is PNIPAM. The LCST of PNIPAM is close to 32 °C [18]. With change in temperature, PNIPAM chains undergo reversible expansion and contraction. At its LCST, PNIPAM undergoes a phase transition. It exhibits hydrophilicity and swells below its LCST. However, it displays hydrophobicity and undergoes deswelling above its LCST [19]. Ye et al. [20] prepared copolymers of polystyrene and poly(*N*-isopropylacrylamide) (PS-b-PNIPAM) and found that the shell of PNIPAM shrinks as the temperature rises from 20 to 40 °C. Lorenzo and coworkers [21] prepared

temperature-sensitive interpenetrating polymer network (IPN) of chitosan and PNIPAM by free radical polymerization. The prepared IPNs were tested as a drug delivery system and found to have good release behavior due the presence of PNIPAM. Burillo et al. [22] prepared grafted hydrogels based on acrylic acid (AAc) and *N*-isopropylacrylamide (NIPAM) on to polypropylene (PP) by gamma radiation. The synthesized hydrogels were utilized for Cu (II) adsorption thus depicting the use of PNIPAM for metal ion adsorption for water cleansing. Garcí a and coworkers [23] prepared graft copolymers of *N*-(3-aminopropyl) methacrylamide hydrochloride (APMA), NIPAM, and polypropylene (PP). The authors reported the LCST of the prepared copolymer to lie near the physiological temperature of human body and concluded that it has potential to be used as a biomedical device.

In the present study, the authors aimed at incorporating biocompatibility of poly(HEMA) and thermo-sensitivity of poly(NIPAM) to produce copolymer cryogels of poly(2-hydroxyethyl methacrylate-*co*-*N*-isopropyl acrylamide) and study their water intake behavior under varying experimental conditions. Although copolymeric gels of HEMA and NIPAM have been prepared earlier by other authors also [24, 25] without following cryogelation technique, the present work aimed at preparing them specifically by cryogelation technique which yields cryogels with macroporous architecture. The prepared cryogels were also characterized by thermal and biocompatibility studies. The swelling behavior and porosity of the gels were also investigated as a function of the concentrations of monomers, cross-linker and redox components, and no of freeze–thaw cycles used in the preparation of the cryogel. Moreover, the effect of swelling medium (pH, temperature, simulated biological fluids) on the extent of swelling and the swelling kinetics were also studied. The structural and network parameters of the cryogels based on swelling studies were also determined.

Experimental

Materials

The monomers 2-hydroxyethyl methacrylate (HEMA) and *N*-isopropylacrylamide (NIPAM) were obtained from Sigma-Aldrich Co. HEMA was purified before use following the procedure described in the literature [26]. NIPAM was used as received. Potassium metabisulfite (KMBS) was obtained from HIMEDIA (New Delhi, India) and used as redox activator. Potassium persulphate (KPS) was used as a redox initiator and *N*, *N*-methylenebisacrylamide (MBA) as a cross-linking agent of the polymers. KPS and MBA were obtained from Research Lab Fine Chem. Industries, Mumbai, India. Other chemicals were of analytical grade, and doubly distilled water was used throughout the experiments.

Methods

Preparation of cryogels

The cryogels were synthesized by the following method: 3.35 mM NIPAM, 8.24 mM HEMA and 0.454 mM MBA as cross-linker were dissolved in 8 mL doubly distilled water. The reaction mixture was cooled in an ice bath for a few minutes. This was followed by addition of 0.359 mM KMBS and 0.036 mM KPS, respectively, and immediately kept for freezing in a petri dish at − 15 °C for 24 h. After 24 h, the contents of the petri dish were thawed. It was observed that the whole reaction mixture converted into a soft, elastic and solid mass. It was further noticed that there were no changes in the appearance and properties of cryogel beyond 24 h which indicated for complete polymerization of vinyl monomers. The soft elastic mass thus formed was named as P(HEMA-*co*-NIPAM) cryogel. Another cryogel having composition as 8.24 mM HEMA, 0.454 mM MBA, 0.359 mM of KMBS, 0.036 mM of KPS and 8 mL of bidistilled water was also prepared following the same procedure as described above. This cryogel was named as PHEMA. Any unreacted chemicals remaining in the prepared cryogels were leached out by leaving them in bidistilled water for a week. Water used for leaching the cryogel was refreshed periodically. The leachate was analyzed for the remaining unreacted vinyl monomers following a double bond estimation procedure, and it was found that the leachate did not contain measurable amounts of the unreacted vinyl monomers. The prepared cryogels were left at room temperature for a week for drying and subsequently kept in polythene bags till further use.

Swelling studies

Water imbibitions property of the cryogels was ascertained by subjecting them to swelling studies. The procedure consisted of the following steps: Dry pieces of the cryogel were weighed and immersed in phosphate buffer saline (PBS, pH = 7.4). At definite time intervals, the cryogel pieces were removed from PBS and the excess surface water was removed by gently placing the cryogel pieces in between the two filter papers for few seconds and thereafter finally weighed on a sensitive digital balance (Denver, Germany). This process was repeated until the cryogels reached a constant weight. Percentage equilibrium swelling is calculated by Eq. 1 [27],

$$Percentage\ Equilibrium\ Swelling = \frac{W_s - W_d}{W_d} \times 100 \quad (1)$$

where W_s represents the weight of wet/swollen cryogel and W_d is the weight of the dry cryogel piece.

Porosity determination

Porosity of the prepared cryogels was determined as follows: Dried cryogel pieces were immersed in PBS till they attained an equilibrium swelling. Swollen pieces were weighed and then pressed to squeeze out the water that was held in the pores. After squeezing out the water, the cryogel pieces were again weighed and percentage porosity is calculated by Eq. 2 as given below [28],

$$Percentage\ Porosity \approx \frac{W_{sw} - W_{seq}}{W_{sw}} \times 100 \tag{2}$$

where W_{sw} and W_{seq} are the weights of wet/swollen and squeezed cryogels, respectively.

While synthesizing the copolymers, the concentrations of the monomers (NIPAM, HEMA), cross-linker (MBA) and redox activator and initiator (KMBS and KPS) and the number of freeze–thaw cycles were varied to obtain different compositions of the cryogels. The as-obtained cryogels of different compositions were assessed for their swelling and porosity properties, and a definite composition of cryogel was determined having optimum swelling and porosity. The optimized cryogel was characterized by various analytical techniques, and its water sorption property was studied as a function of pH, temperature, solutes and simulated physiological fluids.

Biocompatibility test (hemolysis test)

Hemolysis test was carried out according to the procedure described elsewhere [27]. The cryogel pieces were immersed in 0.9% NaCl solution (saline solution) till they attained equilibrium swelling. A diluted blood sample was prepared by adding 2 mL of EDTA or acid citrate dextrose (ACD) containing blood to 2.5 mL of saline solution. Now, the pieces of dry cryogels were equilibrated with 10 mL saline solution and added to the diluted blood solution. The blood solution containing cryogel pieces was incubated at 37.5 °C for one h. The suspension was then centrifuged, and the obtained supernatant was measured for its absorbance. The absorbance was determined at 542 nm using a UV–Visible spectrophotometer. A positive control was prepared by mixing 0.2 mL diluted blood sample in 10 mL distilled water, while the negative control was prepared by mixing 0.2 mL diluted blood sample in 10 mL saline solution. Absorbance of positive and negative controls was measured after they were incubated and centrifuged. Percentage hemolysis was calculated with the help of the following equation [27],

$$\%Hemolysis\ ratio = \frac{A_{sample} - A_{negative}}{A_{positive} - A_{negative}} \times 100 \tag{3}$$

where A_{sample}, $A_{negative}$, and $A_{positive}$ are the absorbance of the cryogel sample, negative control and positive control, respectively.

Characterizations

Fourier-transform infrared spectroscopy (FTIR) analysis

The presence of various functional groups in the cryogel was confirmed by FTIR spectroscopy. FTIR spectra of dry P(HEMA-co-NIPAM) cryogel film, purified HEMA and NIPAM monomers were obtained using Shimadzu FTIR spectrophotometer (8400S). Dry thin film of P(HEMA-co-NIPAM) cryogel was mounted on the spectrophotometer, NIPAM monomer was used as a fine powder after mixing with KBr and HEMA monomer was applied in liquid form. All the spectra were generated between 4000 and 450 cm^{-1} at a resolution of 2 cm^{-1}.

Field emission scanning electron microscopy (FESEM) analysis

FESEM images provide topographical information of a material. The surface morphology of P(HEMA-co-NIPAM) cryogels was analyzed by obtaining their FESEM images on Nova Nano FESEM 450. Cryogel pieces were vacuum dried and gold coated using a sputter coater. Dried, gold-coated samples were mounted on the microscope and then analyzed at low vacuum at 20.0 kV. The microscopic images were obtained at 350× and 1000× magnifications.

Thermal analysis

Thermal properties of PHEMA and P(HEMA-*co*-NIPAM) cryogels were determined by carrying out thermogravimetric (TGA) and differential scanning calorimetric (DSC) analysis. The analyses were conducted on Perkin Elmer instrument (STA 8000 and 8500). DSC and TGA thermograms of the cryogels were recorded by heating the samples between 30 °C and 700 °C at a heating rate of 10 °C/min in nitrogen atmosphere.

X-ray diffraction analysis (XRD)

X'pert-pro X-ray diffractometer was used to obtain XRD spectra of PHEMA and P(HEMA-*co*-NIPAM) cryogels. The prepared cryogels were scanned between 5° and 90°, 2θ. The obtained data were plotted after filtration and deconvolution using PeakFit software.

Results and discussion

During synthesis of the copolymers (as described in Methods section), the concentrations of the monomers (NIPAM, HEMA), cross-linker (MBA) and redox activator and initiator (KMBS and KPS), and the number of freeze thaw cycles was varied to obtain different compositions of the cryogels as summarized in

Table 1 Percentage porosity and hemolysis ratio for various compositions of cryogels

S. no	NIPAM (mM)	HEMA (mM)	Molar Ratio (NIPAM/HEMA)	MBA (mM)	KMBS (mM)	KPS (mM)	FTC	% Porosity	% Hemolysis ratio
1	0.0	8.24	0:1	0.454	0.287	0.029	3	69.2	0.28
2	3.35	8.24	0.41:1	0.454	0.287	0.029	3	48.94	0.56
3	4.41	8.24	0.54:1	0.454	0.287	0.029	3	39.47	0.729
4	5.56	8.24	0.67:1	0.454	0.287	0.029	3	20.66	0.841
5	3.35	12.36	0.27:1	0.454	0.287	0.029	3	45.93	0.616
6	3.35	16.48	0.2:1	0.454	0.287	0.029	3	43.9	0.673
7	3.35	20.61	0.16:1	0.454	0.287	0.029	3	31.81	0.785
8	3.35	8.24	0.41:1	0.518	0.287	0.029	3	45.4	0.673
9	3.35	8.24	0.41:1	0.583	0.287	0.029	3	41.17	0.729
10	3.35	8.24	0.41:1	0.648	0.287	0.029	3	37.9	0.785
11	3.35	8.24	0.41:1	0.454	0.179	0.018	3	42.52	0.785
12	3.35	8.24	0.41:1	0.454	0.359	0.036	3	57.2	0.392
13	3.35	8.24	0.41:1	0.454	0.359	0.036	1	62.34	0.336
14	3.35	8.24	0.41:1	0.454	0.359	0.036	2	59.13	0.336
15	3.35	8.24	0.41:1	0.454	0.359	0.036	4	55.45	0.448
16	3.35	8.24	0.41:1	0.454	0.359	0.036	5	51.62	0.504

Table 1. The as-obtained cryogels were assessed by swelling, and porosity studies and the findings are discussed below. It is worth to mention here that among all the compositions mentioned in Table 1, the P(HEMA-*co*-NIPAM) cryogel having the composition [NIPAM] = 3.35 mM, [HEMA] = 8.24 mM, [MBA] = 0.454 mM, [KMBS] = 0.359 mM, [KPS] = 0.036 mM, and number of freezing and thawing cycles (FTC) = 1 exhibited highest percentage of equilibrium swelling and, therefore, was selected as a control for characterization studies.

Swelling and porosity studies

Influence of NIPAM

To assess the impact of NIPAM monomer concentration on swelling performance and porosity of the prepared cryogels, the concentration of NIPAM was changed from 0 mM to 5.56 mM in the reaction mixture. The results are depicted in Fig. 1 and Table 1. It is apparent from the figure and values of the porosity summarized in Table 1 that as the concentration of NIPAM monomer increased in the reaction mixture, the percentage equilibrium swelling and porosity decreased. The cryogel with 8.24 mM HEMA and 0.0 mM NIPAM showed higher swelling as compared to other cryogels that contained NIPAM. Scognamillo and coworkers [29] prepared hydrogels of NIPAM with 3-sulfopropyl acrylate potassium salt and found that with an increase in the molar concentration of NIPAM in the hydrogel, the percentage equilibrium swelling decreased. The observed swelling trend can be justified on the ground that at 37 °C the PNIPAM becomes hydrophobic. Therefore, as the hydrophobic content (NIPAM) increases in the copolymeric chains of the network, the swelling decreases. Furthermore, the –OH groups of HEMA and –NH groups of

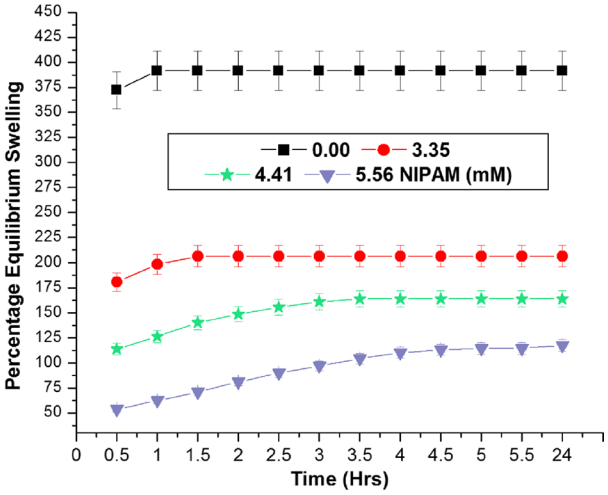

Fig. 1 Influence of varying NIPAM concentration on % equilibrium swelling of cryogel at fixed composition [HEMA] = 8.24 mM, [MBA] = 0.454 mM, [KMBS] = 0.287 mM, [KPS] = 0.029 mM and number of freezing and thawing cycles = 3, Temp = 37 °C

NIPAM resulted in an increased hydrogen bonding as the NIPAM concentration increased. As a consequence, there were lesser number of free hydroxyl or amine groups to participate in hydrogen bond formation with water molecules which results in a lower water uptake. Increased hydrogen bonding between –OH and –NH groups may also have led to the generation of a dense cryogel with thicker walls which are supported by the fact that percentage porosity decreased with increased NIPAM content. Figure 1 also reveals that the increased amount of NIPAM in the cryogel not only resulted in a decrease in percentage equilibrium swelling, but it also took longer time to attain equilibrium swelling.

Influence of HEMA

The influence of HEMA concentration on percentage equilibrium swelling and percentage porosity was also analyzed by varying the concentration of HEMA monomer in the range 8.24 to 20.61 mM in the reaction mixture during synthesis. The results are shown in Fig. 2 and Table 1 which reveal that as the concentration of HEMA rises in the reaction mixture, the percentage equilibrium swelling and porosity decline. As HEMA concentration increases in the copolymer, the hydrophobic interaction between the copolymer chains of the network increases which causes reduced swelling. This observation further corroborates the findings that were described above for the study of influence of NIPAM on equilibrium swelling. Similar to the increase in NIPAM content, the increased concentration of HEMA resulted in greater number of –OH groups available for hydrogen bonding with –NH groups of NIPAM which led to a decrease in swelling of the cryogels. Çiçek et al. [24] reported similar type of results when they prepared copolymers of HEMA and NIPAM by redox polymerization and observed a decrease in

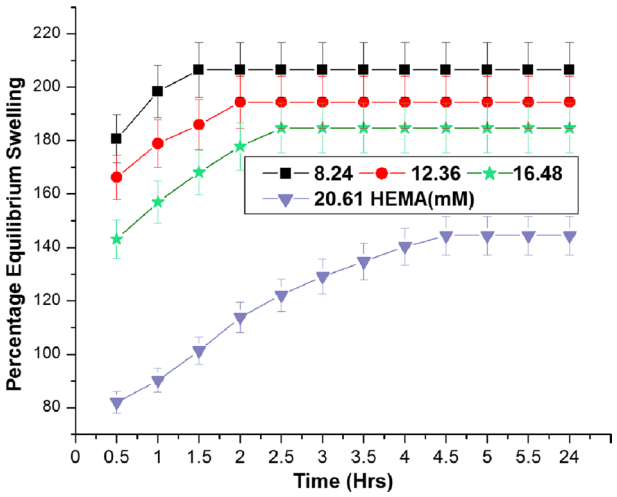

Fig. 2 Influence of varying HEMA concentration on % equilibrium swelling of cryogel at fixed composition [NIPAM] = 3.35 mM, [MBA] = 0.454 mM, [KMBS] = 0.287 mM, [KPS] = 0.029 mM, and number of freezing and thawing cycles = 3, Temp = 37 °C

equilibrium swelling ratio as the amount of HEMA increased in the copolymer. Figure 2 also reveals that cryogels with lower percentage equilibrium swelling take more time to swell. This is further supported by the porosity values which decrease with the increase in HEMA content. The reduced values of porosity are also responsible for the lower water uptake capacity.

Influence of MBA cross-linker

The influence of cross-linker concentration on the percentage equilibrium swelling and percentage porosity was studied by varying the concentration of MBA in the range 0.454 to 0.648 mM in the reaction mixture. The results are depicted in Fig. 3 and Table 1 which indicate a decrease in percentage equilibrium swelling and percentage porosity with increasing concentration of MBA. This observation can be accounted on the grounds that with the increased MBA concentration, there is greater degree of cross-linking between the polymer chains which led to the formation of a dense cryogel with reduced matrix size. Because of the dense network, the flow of water into the cryogel network is hindered and the water uptake capacity of the cryogel also declined. The reduced swelling is also caused by the decreased porosity of the cryogel with increased MBA concentration. Sayil et al. [30] prepared hydrogels of NIPAM using MBA as a cross-linker and observed a drop in the swelling ratio with increasing concentration of MBA. It is also noticed that the cryogels produced with lower concentration of MBA not only have higher swelling but also acquire equilibrium swelling in shorter time as opposed to cryogels with higher content of MBA.

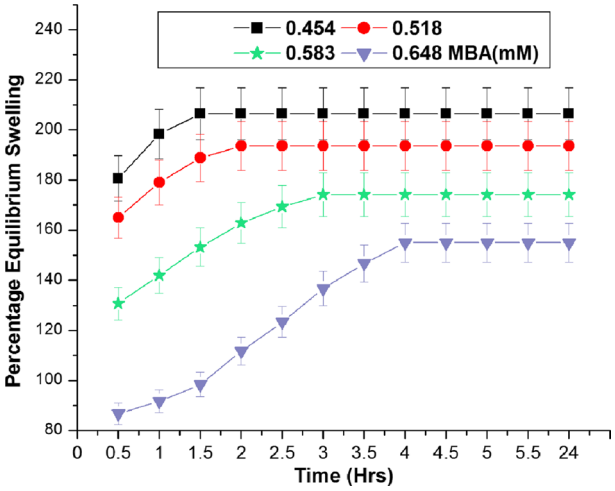

Fig. 3 Influence of varying MBA concentration on % equilibrium swelling of cryogel at fixed composition [NIPAM] = 3.35 mM, [HEMA] = 8.24 mM, [KMBS] = 0.287 mM, [KPS] = 0.029 mM and number of freezing and thawing cycles = 3, Temp = 37 °C

Influence of redox components

The impact of varying concentrations of activator and initiator (KMBS and KPS) of the redox components on percentage equilibrium swelling and percentage porosity was investigated by varying the concentration of KMBS in the range 0.179 to 0.359 mM and that of KPS from 0.018 mM to 0.036 mM in the reaction mixture at the time of synthesis, respectively. It is clear from Fig. 4 and Table 1 that as the concentrations of KMBS and KPS increased in the reaction mixture, the percentage equilibrium swelling and porosity also increased. As the concentrations of the redox activator and initiator increase in the reaction mixture, there are a greater number of monomer molecules converting into free macroradicals at the start of the polymerization process. This subsequently creates a large number of polymer chains with large number of pores in between them. These voids or pores imbibe water during swelling process which results in an elevated equilibrium swelling [31]. This is further confirmed by the increased percentage porosity of the cryogel network with increasing concentrations of redox components. It is also observed that cryogels produced with greater concentration of redox components attained a faster equilibrium swelling because of the presence of large number of pores.

Influence of number of cycles

During the synthesis process of cryogel, the reaction mixture was frozen for 24 h and then defrosted for two h. This constitutes a freezing–thawing cycle. The influence of number of freezing and thawing cycles on percentage equilibrium swelling and percentage porosity was also studied by varying the number of freezing–thawing cycles from 1 to 5. Figure 5 and Table 1 present the obtained results, and the

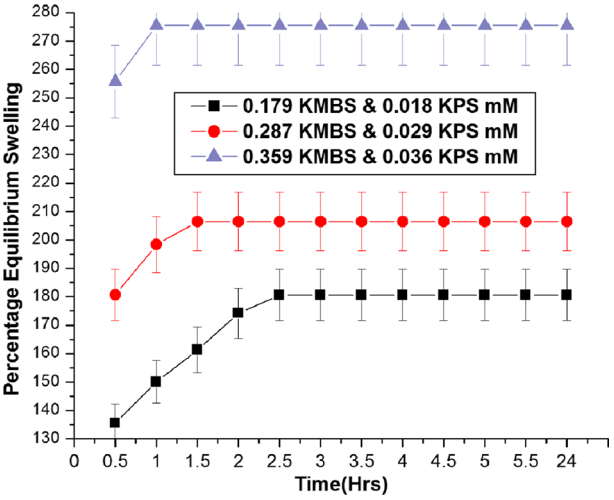

Fig. 4 Influence of varying redox concentration (KMBS and KPS) on % equilibrium swelling of cryogel at fixed concentration [NIPAM] = 3.35 mM, [HEMA] = 8.24 mM, [MBA] = 0.454 mM and number of freezing and thawing cycles = 3, Temp = 37 °C

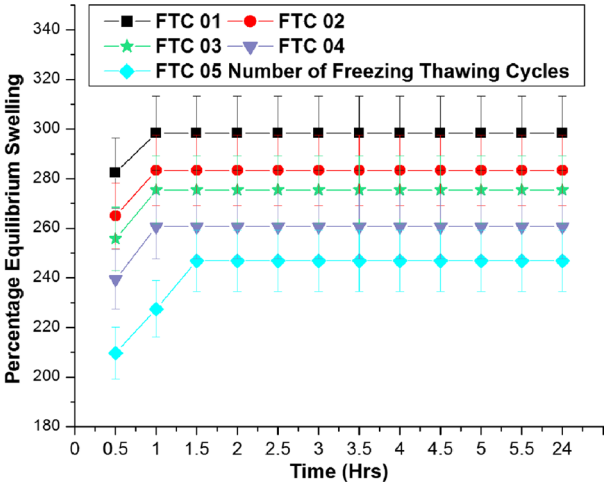

Fig. 5 Influence of varying number of freezing and thawing cycles on % equilibrium swelling of cryogel at fixed composition [NIPAM] = 3.35 mM, [HEMA] = 8.24 mM, [MBA] = 0. 454 mM, [KMBS] = 0.359 mM, [KPS] = 0.036 mM, Temp = 37 °C

results indicate that as the number of freezing–thawing cycles increased, percentage equilibrium swelling and percentage porosity decreased. The degree of cross-linking increased with the increased number of freezing cycles which resulted in the formation of a more compact cryogel with decreased lattice size which results in a slower diffusion of water molecules into the cryogel. The percentage porosity also decreased as the number of freeze–thaw cycles increased and thus the extent of swelling also decreased. However, the observed decrease is quite slight in each cycle. Figure 6 presents the pictures of P(HEMA-*co*-NIPAM) cryogel which show

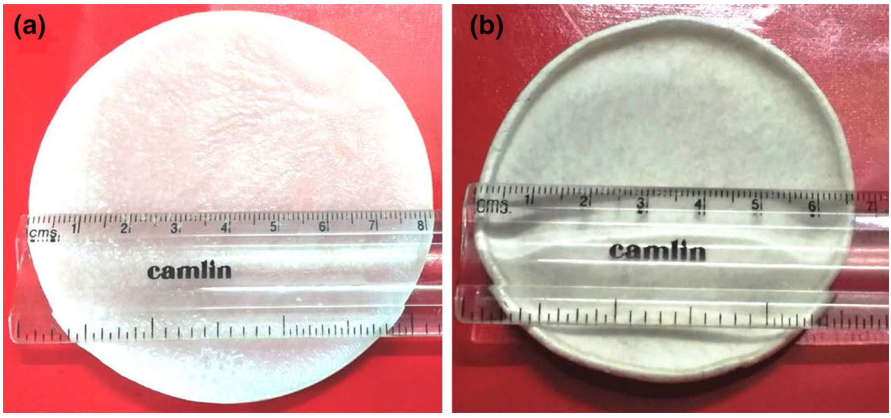

Fig. 6 Images showing the digital photographs of cryogel in **a** swollen state, **b** dry state of P(HEMA-*co*-NIPAM) cryogel of fixed composition [NIPAM] = 3.35 mM, [HEMA] = 8.24 mM, [MBA] = 0.454 mM, [KMBS] = 0.359 mM, [KPS] = 0.036 mM and number of freezing and thawing cycle = 1

highest percentage equilibrium swelling among all the compositions in swollen and dry states.

Influence of pH

The pH of the swelling medium was varied from 1.6 to 8.5 to study its influence on the swelling behavior of cryogel. The obtained findings are presented in Fig. 7 which reveals that the swelling of cryogel is marginally affected by alterations in pH of the swelling medium. Percentage equilibrium swelling increased slightly at pH value of 1.6 and 8.5 as compared to the percentage equilibrium swelling at pH 7.4 (PBS). Non-ionic nature of PHEMA and PNIPAM makes their swelling response independent to the pH of the surrounding medium. The slight increase in swelling at pH value of 1.6 and 8.5 may have been due to breaking of some of the hydrogen bonds in the cryogel network structure at lower and higher pH which resulted in greater imbibition of water. Don and coworkers [32] prepared hydrogels of PNIPAM and found that the swelling behavior of the prepared hydrogels was independent of the pH of the surrounding medium.

Influence of solutes and simulated physiological fluids

Equilibrium swelling is also influenced by the presence of solutes in the surrounding medium. This was studied by immersing P(HEMA-*co*-NIPAM) cryogel in the solutions prepared from KI and urea. Solutions of various simulated physiological fluids such as saline, D-glucose and synthetic urine were also used in this study. The results are presented in Fig. 8 which reveals that the cryogel exhibits higher percentage equilibrium swelling in the presence of PBS as compared to other media. The

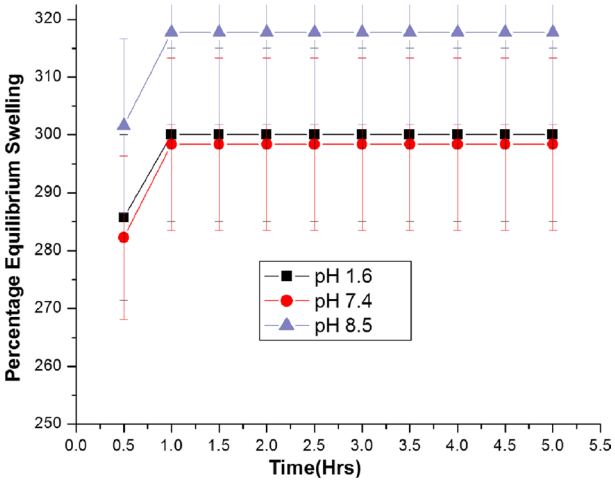

Fig. 7 Influence of varying pH on % equilibrium swelling of cryogel of fixed composition [NIPAM] = 3.35 mM, [HEMA] = 8.24 mM, [MBA] = 0. 454 mM, [KMBS] = 0.359 mM, [KPS] = 0.036 mM, and number of freezing and thawing cycles = 1, Temp = 37 °C

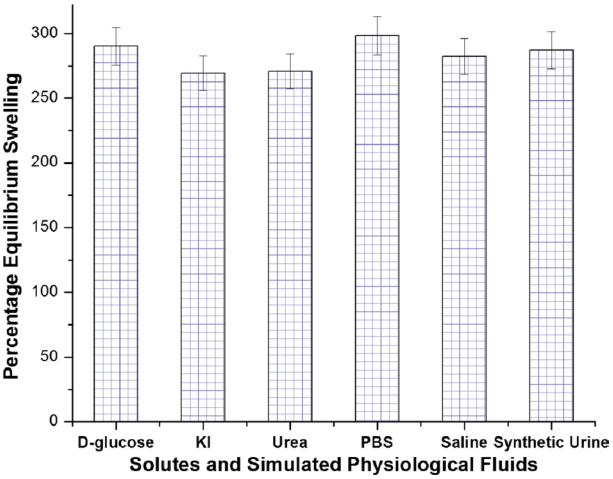

Fig. 8 Influence of varying solutes and simulated physiological fluids on % equilibrium swelling of cryogel of fixed composition [NIPAM] = 3.35 mM, [HEMA] = 8.24 mM, [MBA] = 0.454 mM, [KMBS] = 0.359 mM, [KPS] = 0.036 mM and number of freezing and thawing cycles = 1, Temp = 37 °C

presence of solutes in the swelling medium must have altered the osmotic pressure which caused a reduced swelling.

Influence of temperature

While analyzing polymers based on thermoresponsive monomers such as NIPAM, an essential parameter to be considered is the impact of temperature. Figure 9 represents the influence on percentage equilibrium swelling when the temperature of the swelling medium (PBS) is altered. The temperature was varied from 10 °C to 47 °C, and it was observed that the P(HEMA-*co*-NIPAM) cryogel exhibited highest percentage equilibrium swelling at 10 °C and lowest at 47 °C. Thus, as the temperature increased, the percentage equilibrium swelling declined. This is expected also since the NIPAM undergoes volume phase transition from a hydrophilic state to a hydrophobic state beyond its LCST. As mentioned previously, the LCST of PNIPAM is around 32 °C. However, this value varies when PNIPAM is used in the copolymer form rather than a homopolymer. The value of phase transition temperature and degree of temperature sensitivity depend upon the nature of the monomer with which NIPAM has been copolymerized and its concentration in the copolymer. The term LCST applies to linear polymers of NIPAM; however, the term volume phase transition temperature (VPTT) applies to the cross-linked polymers of NIPAM [33]. The graph (Fig. 9) shows a major decline in swelling after 20 °C. Thus, VPTT for the prepared P(HEMA-*co*-NIPAM) may be determined from the midpoint between 20 °C and 25 °C which is 22.5 °C. The decrease in VPTT may be attributed to the presence of poly(HEMA) in the prepared cryogel. Gan and coworkers [25] synthesized microgels of P(NIPAM-HEMA) and reported the VPTT at 29 °C. They also stated that this value is less by 3 °C as compared to that of the PNIPAM microgels

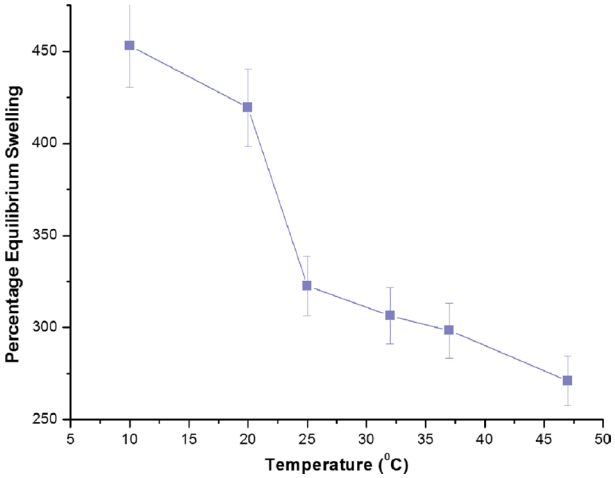

Fig. 9 Influence of temperature on % equilibrium swelling of the cryogel of fixed composition [NIPAM] = 3.35 mM, [HEMA] = 8.24 mM, [MBA] = 0.454 mM, [KMBS] = 0.359 mM, [KPS] = 0.036 mM and number of freezing and thawing cycles = 1

which have VPTT around 32 °C. They explained this decrease in VPTT due to the presence of HEMA which forms hydrogen bonding. The hydroxyl groups (–OH) of HEMA not only form hydrogen bonds among themselves but also get hydrogen bonded with the amide group (–CONH) of NIPAM. This consequently leads to the copolymer exhibiting more hydrophobicity than the homopolymer of pure PNIPAM. This leads to a shifting of the VPTT to the lower side. The impact of temperature on equilibrium swelling was also analyzed with respect to time and is shown in Fig. 10. The results show that although the cryogel exhibited higher swelling at lower temperature, it also took longer time to attain equilibrium swelling. The cryogel showed faster water uptake at higher temperature.

Structural and network parameters

In cross-linked polymers, the average or mean molecular mass (M_c) between the cross-links is a key structural and network factor. Mechanical and physical properties of polymers are greatly dependent on the magnitude of M_c. The ratio of weight of polymer in swollen state to that in the dry state represents the swelling ratio. Flory and Rehner utilized the swelling ratio values in computing M_c. According to them, the M_c can be calculated by the following Eq. 4 [34],

$$M_c = -V_1 d_p \frac{V_s^{\frac{1}{3}} - V_s/2}{\ln\left(1 - V_s\right) + V_s + \chi V_s^2} \tag{4}$$

where V_1 represents the molar volume of solvent (water = 18.02 mL mol^{-1}), V_s stands for volume fraction of polymer in the swollen cryogel, dp is polymer density

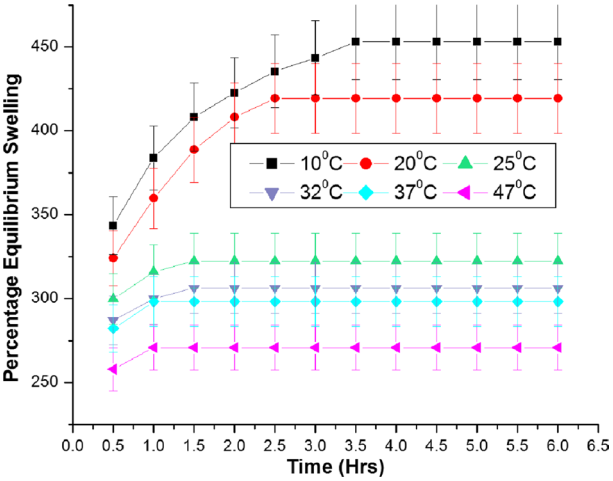

Fig. 10 Influence of varying temperature with time on % equilibrium swelling of the cryogel of fixed composition [NIPAM] = 3.35 mM, [HEMA] = 8.24 mM, [MBA] = 0.454 mM, [KMBS] = 0.359 mM, [KPS] = 0.036 mM and number of freezing and thawing cycles = 1

(g mL^{-1}), χ represents the Flory–Huggins polymer—solvent interaction factor, and V_s is equal to 1/swelling ratio. Another network parameter is cross-linking density which is represented by q and calculated by Eq. 5 [34],

$$q = \frac{M_o}{M_c} \tag{5}$$

where M_0 represents the molar mass of the polymer's repeat unit. The value of M_0, for the prepared copolymeric cryogel, can be determined by Eq. 6 [34],

$$M_o = \frac{n_{NIPAM} M_{NIPAM} + n_{HEMA} M_{HEMA}}{n_{NIPAM} + n_{HEMA}} \tag{6}$$

where n_{NIPAM} and n_{HEMA} represent the number of moles of NIPAM and HEMA, respectively. Molar masses of NIPAM and HEMA are represented by M_{NIPAM} and M_{HEMA} (g mol^{-1}), respectively. Some authors represent cross-linking density by V_e and consider it to be the total number of elastically effective chains present in the polymer network, per unit volume. V_e can be calculated by the equation given below [34],

$$V_e = \frac{d_p N_A}{M_C} \tag{7}$$

where N_A stands for Avogadro's number. Pycnometry was used to determine the polymer density (d_p). The polymer and solvent interaction factor χ was calculated by Eq. 8 [35],

$$\chi \approx \frac{1}{2} + \frac{V_s}{3} \tag{8}$$

Using Eqs. (4–8) the values of M_c, V_e and q were determined for various compositions of the cryogels and are summarized in Table 2.

Biocompatibility test (hemolysis test)

Table 1 summarizes the results of hemolysis test. It can concluded from the obtained data that all the compositions of the prepared cryogels showed low value for percentage hemolysis ratio (< 0.9%) thus suggesting for the biocompatible nature of the prepared cryogels. Figure 11 presents the images of the test results. The positive control caused excessive hemolysis, while the negative control and test samples showed negligible hemolysis. Percentage hemolysis for P(HEMA-*co*-NIPAM) cryogel was found to be 0.336% which is within the acceptable limit for a biocompatible material. A material is considered as having high biocompatibility if it has hemolysis value of 5% or less [27].

FTIR analysis

Figure 12a shows the spectrum of HEMA monomer which reveals a broad peak at 3390–3549 cm^{-1} and can be ascribed to the presence of hydrogen bonded hydroxyl (–OH) groups. The presence of carbonyl (–CO) group is affirmed from the peak observed at 1720 cm^{-1}. The –CH stretching vibrations are seen at 2958 cm^{-1}. Besides these, the spectral peaks of HEMA and the peak appeared at 1450 cm^{-1} can be assigned to –CH bending vibrations. The peaks at 1082–1188 cm^{-1} are owing to –C–O–C– stretching vibrations. Figure 12b shows the spectrum of NIPAM monomer. The prominent peaks observed in the spectrum are as follows: the peaks at 1645 cm^{-1}, 1545 cm^{-1} are caused due to –C=O stretching (Amide I) and –NH bending (Amide II) vibrations, respectively. These two peaks can be attributed to the vibrations of the amide group (–CO–NH). The peaks at 2972 cm^{-1} can be attributed to –CH stretching vibrations while that at 1458 cm^{-1} is due to –CH bending vibrations. The presence of isopropyl group (–CH $(CH_3)_2$) is observed as a twin peak at 1309 cm^{-1} and 1328 cm^{-1}. The peak at 3313 cm^{-1} is due to –NH stretching vibrations. The spectrum of P(HEMA-*co*-NIPAM) cryogel is seen in Fig. 12c, and it confirms the presence of NIPAM and HEMA monomers in the prepared cryogel. The broad peak ranging from 3475 cm^{-1} to 3666 cm^{-1} can be ascribed to the vibrations of –NH and –OH groups. The –CO stretching vibrations of HEMA can be seen as a sharp peak at 1743 cm^{-1}. The peaks at 1668 cm^{-1} (–C=O stretching of Amide I) and 1562 cm^{-1} (–NH bending of Amide II) can be attributed to the vibrations of the amide group (–CO–NH). The peak at 2997 cm^{-1} is owing to the –CH stretching vibrations. The peak at 1398 cm^{-1} can be assigned to the isopropyl group (–CH $(CH_3)_2$) of NIPAM. In addition, the spectrum (c) also shows peaks at 1492 cm^{-1} and 1093–1193 cm^{-1} which are assigned to –CH bending and –C–O–C– stretching vibrations, respectively. FTIR spectra of PHEMA and PNIPAM polymers with similar findings are reported in the literature [36, 37].

Table 2 Various compositions of cryogels and their respective network parameters

S. no.	NIPAM (mM)	HEMA (mM)	Molar ratio (NIPAM/HEMA)	MBA (mM)	KMBS (mM)	KPS (mM)	Freezing–Thawing cycles (FTC)	Average molar mass (M_C) (g mol^{-1})	Cross-link density (q)	Elastically effective chains (V_e)$\times 10^{-19}$
1	0.0	8.24	0:1	0.454	0.287	0.029	3	12,332.84	0.01	3.51
2	3.35	8.24	0.41:1	0.454	0.287	0.029	3	2087.4	0.059	24.52
3	4.41	8.24	0.54:1	0.454	0.287	0.029	3	1291.68	0.096	46.62
4	5.56	8.24	0.67:1	0.454	0.287	0.029	3	707.66	0.174	110.64
5	3.35	12.36	0.27:1	0.454	0.287	0.029	3	1883.17	0.067	29.1
6	3.35	16.48	0.2:1	0.454	0.287	0.029	3	1704.64	0.074	33.56
7	3.35	20.61	0.16:1	0.454	0.287	0.029	3	1107.25	0.115	65.27
8	3.35	8.24	0.41:1	0.518	0.287	0.029	3	1863.7	0.067	29.4
9	3.35	8.24	0.41:1	0.583	0.287	0.029	3	1494.89	0.083	39.48
10	3.35	8.24	0.41:1	0.648	0.287	0.029	3	1256.43	0.099	54.16
11	3.35	8.24	0.41:1	0.454	0.179	0.018	3	1602.12	0.078	35.71
12	3.35	8.24	0.41:1	0.454	0.359	0.036	3	4126.9	0.03	10.5
13	3.35	8.24	0.41:1	0.454	0.359	0.036	1	5120.02	0.024	8.23
14	3.35	8.24	0.41:1	0.454	0.359	0.036	2	4497.14	0.027	9.64
15	3.35	8.24	0.41:1	0.454	0.359	0.036	4	3642.94	0.034	12.4
16	3.35	8.24	0.41:1	0.454	0.359	0.036	5	3177.82	0.039	14.59

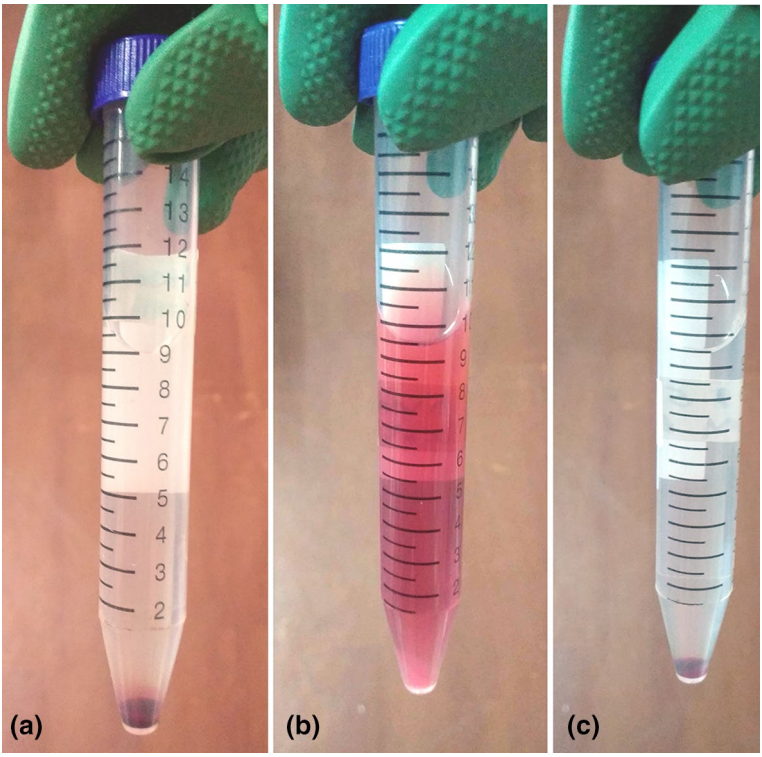

Fig. 11 Images of hemolysis test. **a** P(HEMA-*co*-NIPAM) cryogel, **b** positive control **c** negative control

FESEM analysis

The FESEM images of P(HEMA-*co*-NIPAM) cryogels were obtained at magnifications of 350× and 1000× and are shown in Fig. 13a, b, respectively. The images of the prepared cryogel reveal the surface structure with pore sizes ranging from 11 to 111 µm. The pore walls appear to be quite thick and rough. The pores seem to be distributed unevenly on the surface and are not uniformly cylindrical. Surfaces with pore sizes less than 2 nm (0.002 µm) are termed as micropores, those with pore size more than 50 nm (0.05 µm) are termed as macroporous, and those between 2 to 50 nm are known as mesoporous [38]. Based on this classification, it may be conclude that P(HEMA-co-NIPAM) cryogels can be regarded as macroporous.

DSC analysis

Figure 14a depicts the DSC thermogram of the prepared P(HEMA) cryogels. The glass transition temperature (T_g) of the prepared PHEMA cryogel was found to be 110 °C. The T_g value of PHEMA is reported to be 100–110 °C [39, 40]. The T_g

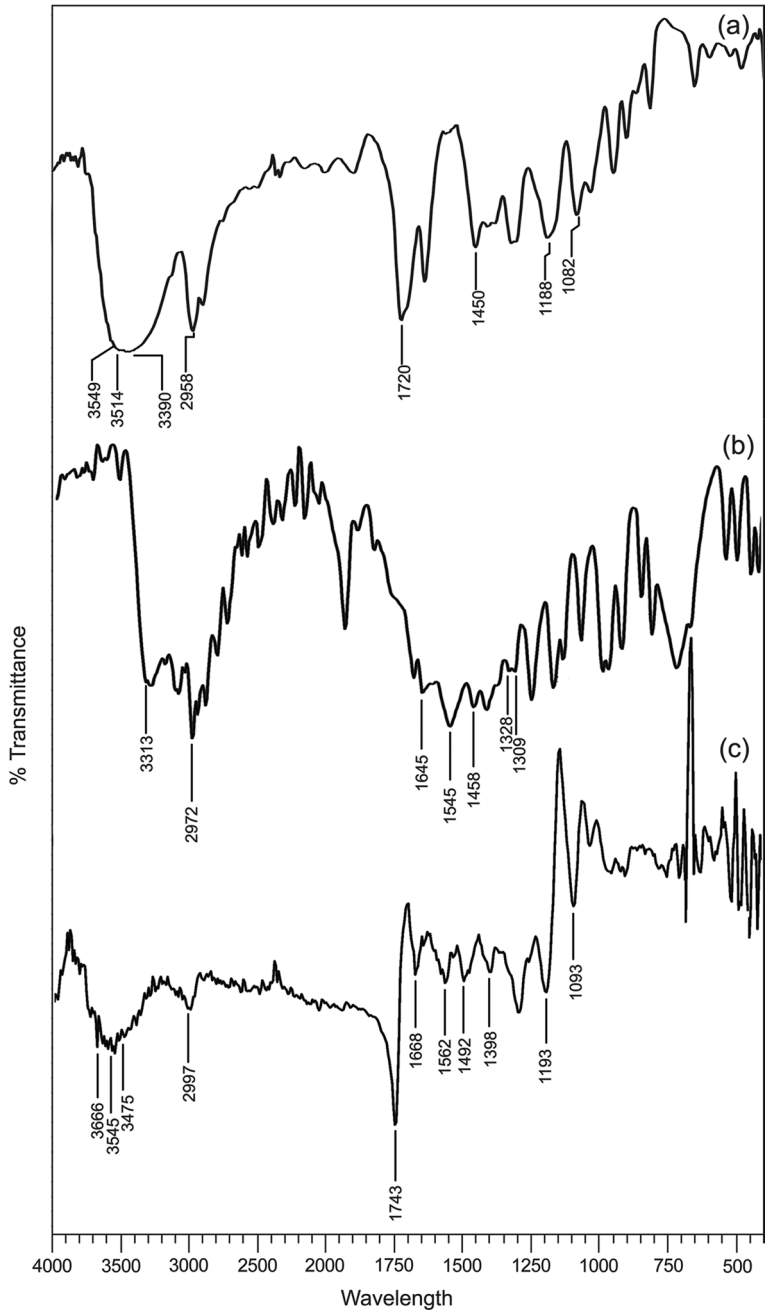

Fig. 12 FTIR spectrums of **a** HEMA monomer, **b** NIPAM monomer, **c** P(HEMA-*co*-NIPAM) cryogel

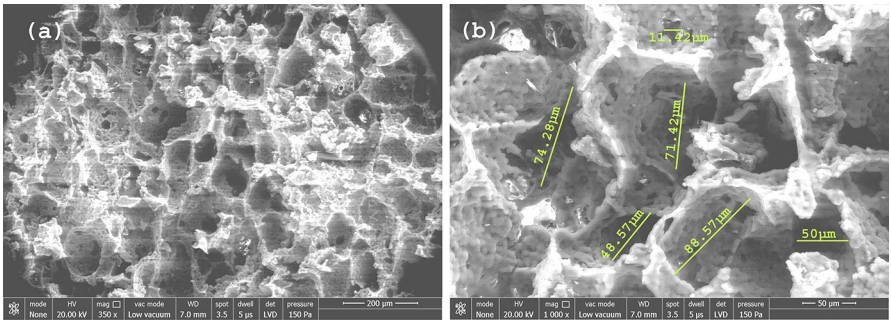

Fig. 13 FESEM images of P(HEMA-*co*-NIPAM) cryogel at **a** 350×, **b** 1000× magnification

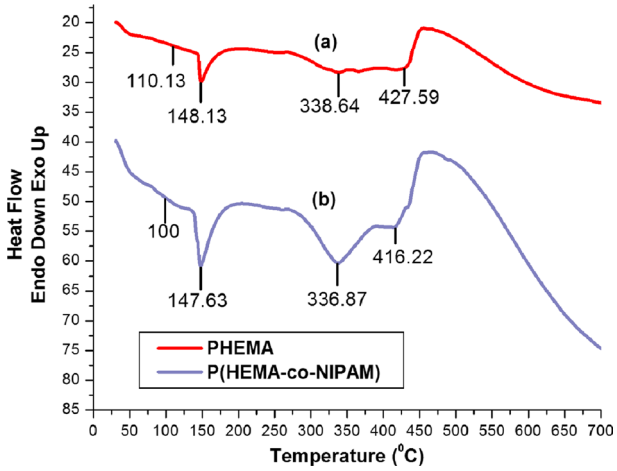

Fig. 14 DSC thermograms of **a** PHEMA cryogel, **b** P(HEMA-*co*-NIPAM) cryogel

of PHEMA was reported at 85 °C by Kajiwara and coworkers [9] who synthesized PHEMA by microwave irradiation technique without using any cross-linker. Katiyar and coworkers [41] prepared PHEMA using propylene glycol dimethacrylate (PGDMA) as a cross-linker and found the T_g at 110 °C. A sharp endotherm is also observed with a peak centered at 148 °C, with an onset around 145 °C and ending at around 175 °C. This may be attributed to the evaporation of residual water in the cryogel. Endothermic peaks associated with loss of water in the range of 70–160 °C and 75–140 °C have been reported in DSC and TGA thermograms of PHEMA and its copolymers by other authors also [42, 43]. Two small endotherms are also noticed at 338 °C and 427 °C, respectively, which may be ascribed to the initial decomposition of the polymer followed by more extensive degradation at 427 °C. Figure 14b depicts the DSC curve of P(HEMA-*co*-NIPAM) copolymer. It is evident from the graph that the T_g of the polymer is observed at 100 °C. Garcí a-Uriostegui and coworkers [44] synthesized polymers based on poly(*N*-isopropylacrylamide) by

ionizing radiation and reported the T_g of PNIAM at 86 °C. The shift in T_g of the synthesized P(HEMA-*co*-NIPAM) cryogel may be due to the combined presence of HEMA, NIPAM, and the cross-linker. This is further followed by an endotherm with an onset temperature at about 134 °C ending at around 180 °C with a peak centered value at 147 °C. It represents the loss of residual water present in the prepared cryogel. The next observed endotherm has an onset at 280 °C with a peak value centered at 336 °C ending around 390 °C. Another small endotherm is observed at 416 °C. These two endotherms can be ascribed to the decomposition of the P(HEMA-*co*-NIPAM) cryogel. The findings of DSC curves are further corroborated by TGA analysis as discussed below.

TGA analysis

Figure 15a represents the TGA thermogram of PHEMA cryogel. The weight loss of PHEMA cryogel can be seen in three zones. The first region of weight loss is observed around 143 °C, and it is ascribed to the loss of water from the cryogel. The second region of weight loss is observed between 300 °C and 400 °C which reveals about 10% weight loss at 300 °C. This represents the onset of thermal degradation which is followed by the third weight loss region starting from 400 °C and continuing till 445 °C. This is also confirmed by DSC data where two degradation endotherms were observed at 338 °C and 427 °C, respectively. Das and coworkers [45] synthesized cross-linked polymers of dextrin with poly(HEMA) and observed several zones of weight losses. The authors attributed one of the regions of weight loss to the degradation of MBA cross-linker and the second region due to the degradation of PHEMA chains. Decomposition temperature of PHEMA polymer has been reported between 337 °C and 480 °C [46]. Figure 15b depicts the TGA thermogram of P(HEMA-*co*-NIPAM) cryogel. The first region of weight loss is observed around 138 °C that may be due to the

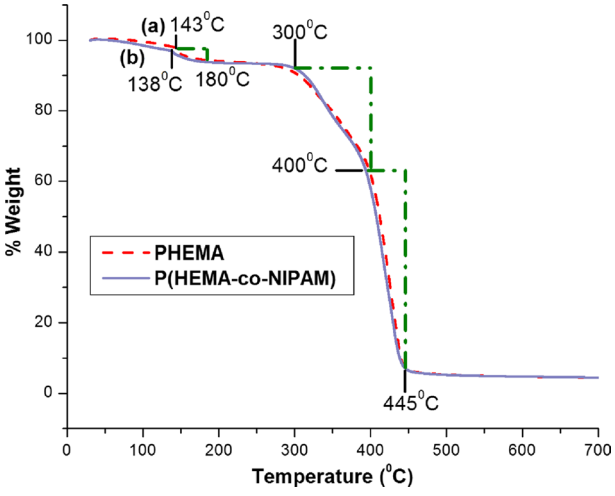

Fig. 15 TGA thermograms of **a** PHEMA cryogel, **b** P(HEMA-*co*-NIPAM) cryogel

evaporation of residual water contained in the cryogel. The thermogram of P(HEMA-*co*-NIPAM) also shows two regions of degradation. The first region of degradation starts at 300 °C and continues up to 400 °C. There is weight loss of about 8% at 300 °C, and it represents the onset of thermal degradation. The second zone of degradation lies between 400 °C to 445 °C. Garcı´a-Uriostegui [44] reported 10% weight loss of PNIPAM polymer at 375 °C. Maximum degradation temperature for PNIPAM cross-linked with MBA has been reported at 407 °C elsewhere [47]. Thus, the TGA results of P(HEMA-*co*-NIPAM) cryogels are in agreement with those reported for PHEMA and PNIPAM. Moreover, the weight loss of only 8% till 300 °C indicates that P(HEMA-*co*-NIPAM) cryogel possesses high thermal stability.

X-ray diffraction analysis (XRD)

Figure 16a represents the XRD diffraction pattern of PHEMA cryogel. It is apparent from the figure that the major diffraction peaks are observed at 2θ angles of 7.88°, 12.57°, 18.48° and 28.54°, respectively. Figure 16b depicts the diffraction pattern of P(HEMA-*co*-NIPAM) and shows diffraction peaks at 2θ angle of 6.53°, 9.32°, 12.05°, 15.09°, 18.37° and 28.66°. The crystallinity index and grain size were also calculated for both the prepared cryogels. Equation 9 [48] represents the Debye–Scherrer equation that was used to calculate the grain size,

$$d = \frac{k\lambda}{\beta \mathrm{Cos}\theta} \tag{9}$$

where d represents the grain size, k is Scherrer constant (0.9), β is diffraction broadening and λ being the wavelength of X-rays (1.54 Å). The grain sizes were determined to be 1.33 nm and 1.95 nm for PHEMA and P(HEMA-co-NIPAM), respectively. Crystallinity index was calculated using Eq. 10 [49],

$$\textit{Crystallinity index} = \frac{I_{\mathrm{cy}} - I_{\mathrm{am}}}{I_{\mathrm{cy}}} \times 100 \tag{10}$$

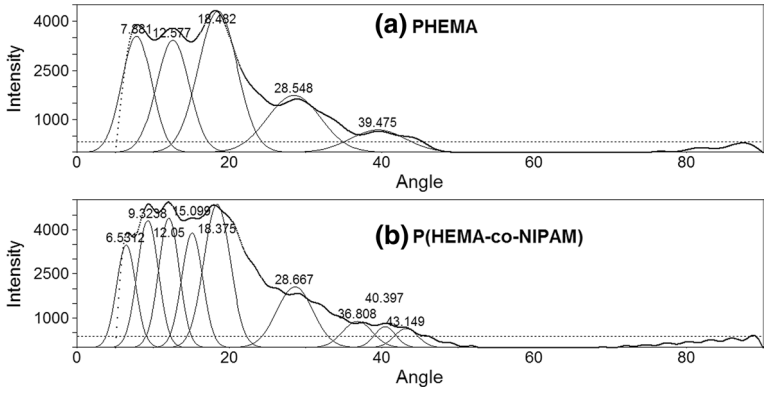

Fig. 16 XRD diffractograms of **a** PHEMA cryogel, **b** P(HEMA-*co*-NIPAM) cryogel

where I_{cy} and I_{am} represent the intensity of the peaks with highest and least intensities in the diffractograms, respectively. The crystallinity indices were calculated to be 84.12% and 86.70% for PHEMA and P(HEMA-*co*-NIPAM), respectively.

Conclusions

HEMA and NIPAM monomers are copolymerized by redox polymerization method in the presence of MBA cross-linker following a cryogelation technique to produce P(HEMA-*co*-NIPAM) cryogels. Fourier-transform infrared spectroscopy (FTIR) spectra of P(HEMA-co-NIPAM) show the characteristic peaks of HEMA and NIPAM monomers thereby confirming the presence of both the monomers in the synthesized cryogel. The surface morphology shows the presence of macropores having pore sizes in the range of 11 to 111 μm. The results of differential scanning calorimetry (DSC) studies reveal two thermal decomposition temperatures at 336 °C and 416 °C which is further confirmed by TGA analysis which reveals decomposition temperature in the range of 300 °C to 445 °C. The prepared cryogels are thermally stable also as indicated by the high decomposition point and only 8% weight loss till 300 °C. Crystallinity index of the cryogel is determined to be 86.70%. P(HEMA-*co*-NIPAM) cryogels having different compositions are prepared, and their percentage equilibrium swelling and porosity are determined with respect to monomers (HEMA and NIPAM), MBA, redox system, and the number of freeze–thaw cycles. It is found that as the concentration of NIPAM, HEMA, MBA and the number of freezing and thawing cycles increase during the synthesis process, percentage equilibrium swelling and porosity decrease which results in the reduction in swelling capacity of the cryogels. However, with increased concentration of redox components, the percentage equilibrium swelling and porosity also show an increment. Equilibrium swelling of P(HEMA-*co*-NIPAM) cryogel is slightly higher at pH 1.6 and 8.5 in contrast to its value at pH 7.4. When the cryogel is immersed in solutions prepared from various solutes and simulated physiological fluids, it displays a diminished swelling value. Thermo-sensitivity due the presence of NIPAM monomer is retained in P(HEMA-co-NIPAM) cryogel also. It shows higher swelling at lower temperature (10 °C), and the swelling declines as the temperature increases. It shows a major decline in swelling after 20 °C. The prepared cryogel is found to be biocompatible as it has hemolysis value of 0.336% only. Thus, from the observed results it may be concluded that P(HEMA-*co*-NIPAM) cryogel is macroporous and has good water sorption capability, thermal stability and biocompatibility. Based on these bio-physical properties, it can be submitted that P(HEMA-*co*-NIPAM) has the potential to be utilized in some biomedical applications such as tissue engineering.

Compliance with ethical standards

Conflict of interest The authors declare that they have no conflict of interest.

References

1. Bencherif SA, Sands RW, Bhatta D et al (2012) Injectable preformed scaffolds with shape-memory properties. Proc Natl Acad Sci 109:19590–19595. https://doi.org/10.1073/pnas.1211516109
2. Lozinsky VI, Galaev IY, Plieva FM et al (2003) Polymeric cryogels as promising materials of biotechnological interest. Trends Biotechnol 21:445–451. https://doi.org/10.1016/j.tibtech.2003.08.002
3. Stanescu MD, Fogorasi M, Shaskolskiy BL et al (2010) New potential biocatalysts by laccase immobilization in PVA cryogel type carrier. Appl Biochem Biotechnol 160:1947–1954. https://doi.org/10.1007/s12010-009-8755-0
4. Belyaeva AV, Smirnova YA, Lysogorskaya EN et al (2008) Biocatalytic properties of thermolysin immobilized on polyvinyl alcohol cryogel. Russ J Bioorg Chem 34:435–441. https://doi.org/10.1134/S1068162008040079
5. Luding Y, Shaochuan S, Junxian Y, Kejian YAO (2011) Isolation of lysozyme from chicken egg white using polyacrylamide-based cation-exchange cryogel. Chin J Chem Eng 19:876–880
6. Sharma A, Bhat S, Vishnoi T et al (2013) Three-dimensional supermacroporous carrageenan-gelatin cryogel matrix for tissue engineering applications. Biomed Res Int 2013:1–15. https://doi.org/10.1155/2013/478279
7. Dainiak MB, Allan IU, Savina IN et al (2010) Gelatin–fibrinogen cryogel dermal matrices for wound repair: preparation, optimisation and in vitro study. Biomaterials 31:67–76. https://doi.org/10.1016/j.biomaterials.2009.09.029
8. Sahiner N, Seven F (2014) The use of superporous p(AAc (acrylic acid)) cryogels as support for Co and Ni nanoparticle preparation and as reactor in H_2 production from sodium borohydride hydrolysis. Energy 71:170–179. https://doi.org/10.1016/j.energy.2014.04.031
9. Kajiwara Y, Nagai A, Chujo Y (2009) Microwave-assisted synthesis of poly(2-hydroxyethyl methacrylate) (HEMA)/silica hybrid using in situ polymerization method. Polym J 41:1080–1084. https://doi.org/10.1295/polymj.PJ2009157
10. Singh B, Dhiman A (2015) Designing bio-mimetic moxifloxacin loaded hydrogel wound dressing to improve antioxidant and pharmacology properties. RSC Adv 5:44666–44678. https://doi.org/10.1039/C5RA06857F
11. Gibas I, Janik H (2010) Synthetic polymer hydrogels for biomedical applications. Chem Chem Technol 4:297–304
12. Al-Shohani A, Awwad S, Tee Khaw P, Brocchini S (2017) The preparation of HEMA-MPC films for ocular drug delivery. Br J Pharm 2:1–11. https://doi.org/10.5920/bjpharm.2017.05
13. Sanyasi S, Kumar A, Goswami C et al (2014) A carboxy methyl tamarind polysaccharide matrix for adhesion and growth of osteoclast-precursor cells. Carbohydr Polym 101:1033–1042. https://doi.org/10.1016/j.carbpol.2013.10.047
14. Ingavle GC, Baillie LWJ, Zheng Y et al (2015) Affinity binding of antibodies to supermacroporous cryogel adsorbents with immobilized protein A for removal of anthrax toxin protective antigen. Biomaterials 50:140–153. https://doi.org/10.1016/j.biomaterials.2015.01.039
15. Erzengin M, Ünlü N, Odabaşı M (2011) A novel adsorbent for protein chromatography: supermacroporous monolithic cryogel embedded with Cu^{2+}-attached sporopollenin particles. J Chromatogr A 1218:484–490. https://doi.org/10.1016/j.chroma.2010.11.074
16. Ward MA, Georgiou TK (2011) Thermoresponsive polymers for biomedical applications. Polymers 3:1215–1242. https://doi.org/10.3390/polym3031215
17. Wei M, Gao Y, Li X, Serpe MJ (2017) Stimuli-responsive polymers and their applications. Polym Chem 8:127–143. https://doi.org/10.1039/C6PY01585A
18. Cappelletti AL, Paez JI (2011) Strumia MC (2011) Synthesis and characterization of thermo-sensitive magnetic maghemite nanoparticles. Ark Online J Org Chem 7:426–438
19. Chang C, Wei H, Wu D-Q et al (2011) Thermo-responsive shell cross-linked PMMA-b-P(NIPAAm-co-NAS) micelles for drug delivery. Int J Pharm 420:333–340. https://doi.org/10.1016/j.ijpharm.2011.08.038
20. Ye X, Fei J, Guan J et al (2010) Dispersion of polystyrene inside polystyrene- *b* -poly(*N* -isopropylacrylamide) micelles in water. J Polym Sci Part B Polym Phys 48:749–755. https://doi.org/10.1002/polb.21948
21. Alvarez-Lorenzo C, Concheiro A, Dubovik AS et al (2005) Temperature-sensitive chitosan-poly(*N*-isopropylacrylamide) interpenetrated networks with enhanced loading capacity and controlled release properties. J Controlled Release 102:629–641. https://doi.org/10.1016/j.jconrel.2004.10.021

22. Burillo G, Castillo-Rojas S, Arrieta H (2012) Cu(II) immobilization in AAc/NIPAAm-based polymer systems synthesized using ionizing radiation. Radiat Phys Chem 81:278–283. https://doi.org/10.1016/j.radphyschem.2011.11.010
23. Contreras-García A, Alvarez-Lorenzo C, Concheiro A, Bucio E (2010) PP films grafted with *N*-isopropylacrylamide and *N*-(3-aminopropyl) methacrylamide by γ radiation: synthesis and characterization. Radiat Phys Chem 79:615–621. https://doi.org/10.1016/j.radphyschem.2009.12.007
24. Çiçek H, Tuncel A (1998) Preparation and characterization of thermoresponsive isopropylacrylamide–hydroxyethylmethacrylate copolymer gels. J Polym Sci Part Polym Chem 36:527–541. https://doi.org/10.1002/(SICI)1099-0518(199803)36:4%3c527:AID-POLA3%3e3.0.CO;2-M
25. Gan T, Zhang Y, Guan Y (2009) In situ gelation of P(NIPAM-HEMA) microgel dispersion and its applications as injectable 3d cell scaffold. Biomacromol 10:1410–1415. https://doi.org/10.1021/bm900022m
26. Bajpai AK, Mishra DD (2004) Adsorption of a blood protein on to hydrophilic sponges based on poly(2-hydroxyethyl methacrylate). J Mater Sci Mater Med 15:583–592
27. Sahiner N, Sagbas S, Sahiner M, Silan C (2017) P(TA) macro-, micro-, nanoparticle-embedded super porous p(HEMA) cryogels as wound dressing material. Mater Sci Eng C 70:317–326. https://doi.org/10.1016/j.msec.2016.09.025
28. Ertürk G, Mattiasson B (2014) Cryogels-versatile tools in bioseparation. J Chromatogr A 1357:24–35. https://doi.org/10.1016/j.chroma.2014.05.055
29. Scognamillo S, Alzari V, Nuvoli D et al (2011) Thermoresponsive super water absorbent hydrogels prepared by frontal polymerization of *N*-isopropyl acrylamide and 3-sulfopropyl acrylate potassium salt. J Polym Sci Part Polym Chem 49:1228–1234. https://doi.org/10.1002/pola.24542
30. Sayil C, Okay O (2001) Macroporous poly(*N*-isopropyl) acrylamide networks: formation conditions. Polymer 42:7639–7652
31. Chen Y-C, Chirila TV, Russo AV (1993) Hydrophilic sponges based on 2-hydroxyethyl methacrylate. II: effect of monomer mixture composition on the equilibrium water content and swelling behaviour. In: Materials forum. Institute of Metals and Materials Australasia, pp 57–65
32. Don T-M, Chou S-C, Cheng L-P, Tai H-Y (2011) Cellular compatibility of copolymer hydrogels based on site-selectively-modified chitosan with poly(*N*-isopropyl acrylamide). J Appl Polym Sci 120:1–12. https://doi.org/10.1002/app.32806
33. Constantin M, Cristea M, Ascenzi P, Fundueanu G (2011) Lower critical solution temperature versus volume phase transition temperature in thermoresponsive drug delivery systems. Express Polym Lett 5:839–848. https://doi.org/10.3144/expresspolymlett.2011.83
34. Bajpai A (2005) Blood protein adsorption onto a polymeric biomaterial of polyethylene glycol and poly[(2-hydroxyethyl methacrylate)-co-acrylonitrile] and evaluation of in vitro blood compatibility. Polym Int 54:304–315. https://doi.org/10.1002/pi.1673
35. Rapado M, Peniche C (2015) Synthesis and characterization of pH and temperature responsive poly(2-hydroxyethyl methacrylate-co-acrylamide) hydrogels. Polímeros 25:547–555. https://doi.org/10.1590/0104-1428.2097
36. Nita LE, Chiriac AP, Nistor M, Budtova T (2013) Upon the delivery properties of a polymeric system based on poly(2-hydroxyethyl methacrylate) prepared with protective colloids. J Biomater Nanobiotechnol 04:357–364. https://doi.org/10.4236/jbnb.2013.44045
37. Lencina MMS, Ciolino AE, Andreucetti NA, Villar MA (2015) Thermoresponsive hydrogels based on alginate-g-poly(*N*-isopropylacrylamide) copolymers obtained by low doses of gamma radiation. Eur Polym J 68:641–649. https://doi.org/10.1016/j.eurpolymj.2015.03.071
38. Solano-Umaña V, Vega-Baudrit JR (2015) Micro, meso and macro porous materials on medicine. J Biomater Nanobiotechnol 06:247–256. https://doi.org/10.4236/jbnb.2015.64023
39. Sun Y-M, Lee H-L (1996) Sorption/desorption properties of water vapour in poly(2-hydroxyethyl methacrylate): 1. Experimental and preliminary analysis. Polymer 37:3915–3919
40. Yang S, Ford J, Ruengruglikit C et al (2005) Synthesis of photoacid crosslinkable hydrogels for the fabrication of soft, biomimetic microlens arrays. J Mater Chem 15:4200–4202. https://doi.org/10.1039/b509077f
41. Katiyar R, Bag DS, Nigam I (2014) Synthesis and evaluation of swelling characteristics of fullerene (C60) containing cross-linked poly(2-hydroxyethyl methacrylate) hydrogels. Adv Mater Lett 5:214–222. https://doi.org/10.5185/amlett.2013.8532
42. Fecchio BD, Valandro SR, Neumann MG, Cavalheiro CCS (2016) Thermal decomposition of polymer/montmorillonite nanocomposites synthesized in situ on a clay surface. J Braz Chem Soc 27:278–284. https://doi.org/10.5935/0103-5053.20150216

43. Podkoscielna B, Bartnicki A, Gawdzik B (2012) New crosslinked hydrogels derivatives of 2-hydroxyethyl methacrylate: synthesis, modifications and properties. Express Polym Lett 6:759–771. https://doi.org/10.3144/expresspolymlett.2012.81
44. García-Uriostegui L, Burillo G, Bucio E (2012) Synthesis and characterization of thermosensitive interpenetrating polymer networks based on *N*-isopropylacrylamide/*N*-acryloxysuccinimide, crosslinked with polylysine, grafted onto polypropylene. Radiat Phys Chem 81:295–300. https://doi.org/10.1016/j.radphyschem.2011.11.053
45. Das D, Das R, Ghosh P et al (2013) Dextrin cross linked with poly(HEMA): a novel hydrogel for colon specific delivery of ornidazole. RSC Adv 3:25340–25350. https://doi.org/10.1039/c3ra44716b
46. Gils PS, Ray D, Sahoo PK (2010) Controlled release of doxofylline from biopolymer based hydrogels. Am J Biomed Sci 2:373–383. https://doi.org/10.5099/aj100400373
47. Hebeish A, Farag S, Sharaf S, Shaheen TI (2014) Thermal responsive hydrogels based on semi interpenetrating network of poly(NIPAm) and cellulose nanowhiskers. Carbohydr Polym 102:159–166. https://doi.org/10.1016/j.carbpol.2013.10.054
48. Bundela H, Bajpai AK (2008) Designing of hydroxyapatite-gelatin based porous matrix as bone substitute: correlation with biocompatibility aspects. Express Polym Lett 2:201–213. https://doi.org/10.3144/expresspolymlett.2008.25
49. Rambo MKD, Ferreira MMC (2015) Determination of cellulose crystallinity of banana residues using near infrared spectroscopy and multivariate analysis. J Braz Chem Soc 26:1491–1499. https://doi.org/10.5935/0103-5053.20150118